

Sivers Effect in Drell-Yan processes

M. Anselmino,¹ M. Boglione,¹ U. D'Alesio,^{2,3} S. Melis,⁴ F. Murgia,³ and A. Prokudin⁴

¹*Dipartimento di Fisica Teorica, Università di Torino and INFN, Sezione di Torino,
Via P. Giuria 1, I-10125 Torino, Italy*

²*Dipartimento di Fisica, Università di Cagliari, I-09042 Monserrato (CA), Italy*

³*INFN, Sezione di Cagliari, C.P. 170, I-09042 Monserrato (CA), Italy*

⁴*Dipartimento di Fisica Teorica, Università di Torino and INFN, Sezione di Torino,
Via P. Giuria 1, I-10125 Torino, Italy*

(Dated: November 13, 2018)

The Sivers distributions recently extracted from semi-inclusive deep inelastic scattering data [1] are used to compute estimates for Sivers asymmetries in Drell-Yan processes which are being planned at several facilities (RHIC, COMPASS, J-PARC, PAX, PANDA, NICA (JINR) and SPASCHARM (IHEP)). Most of these asymmetries turn out to be large and could allow a clear test of the predicted sign change of the Sivers distributions when active in SIDIS and Drell-Yan processes. This is regarded as a fundamental test of our understanding, within QCD and the factorization scheme, of single spin asymmetries.

PACS numbers: 13.88.+e,13.60.-r,13.85.Qk,13.85.-t

I. INTRODUCTION

The experimental study and theoretical understanding of transverse Single Spin Asymmetries (SSA) has been, and still is, one of the most challenging issues in high energy hadron physics. The original, widespread opinion that hadronic SSAs should be negligible in any high energy process, due to the simple, helicity conserving pQCD and Standard Model elementary dynamics [2], has been proven wrong in a great number of cases, actually in most of the spin measurements so far performed. It often happens that the same approach, based on the collinear QCD factorization scheme at leading twist, which successfully describes unpolarized data, cannot explain the large spin effects observed in the same kinematical regions.

The attempts of explaining the data and reconciling them with pQCD dynamics have produced a much deeper understanding of the nucleon structure, involving partonic intrinsic motion, and much progress in clarifying the mechanism, at the partonic level, responsible for providing the phases and helicity flips necessary for a transverse SSA. Many issues, like the universality of these mechanisms and their correct insertion into a factorized scheme, are still under debate and need further investigation.

We consider here the so-called Sivers asymmetry [3, 4], related to the intrinsic motion of partons inside a transversely polarized proton, according to the distribution

$$\hat{f}_{q/p^\uparrow}(x, \mathbf{k}_\perp) = f_{q/p}(x, k_\perp) + \frac{1}{2} \Delta^N f_{q/p^\uparrow}(x, k_\perp) \mathbf{S} \cdot (\hat{\mathbf{P}} \times \hat{\mathbf{k}}_\perp) \quad (1)$$

$$= f_{q/p}(x, k_\perp) - \frac{2k_\perp}{m_p} f_{1T}^{\perp q}(x, k_\perp) \mathbf{S} \cdot (\hat{\mathbf{P}} \times \hat{\mathbf{k}}_\perp), \quad (2)$$

which gives the number density of unpolarized quarks q (or gluons) with intrinsic transverse momentum \mathbf{k}_\perp inside a transversely polarized proton p^\uparrow , with three-momentum \mathbf{P} and spin polarization vector \mathbf{S} ; $\Delta^N f_{q/p^\uparrow}(x, k_\perp)$, or $f_{1T}^{\perp q}(x, k_\perp)$ following a different common notation [5], is the Sivers function. A coupling of the transverse motion of unpolarized quarks and gluons to the nucleon spin can only be related to their orbital motion, and one expects that the observation of the Sivers asymmetry signals partonic orbital angular momentum [6, 7]. Thus, the Sivers distribution is of very special interest.

A clear observation of a non zero Sivers distribution has been obtained by the HERMES collaboration in Semi-Inclusive Deep Inelastic Scattering processes (SIDIS) [8, 9]. A similar measurement by the COMPASS collaboration has given a result compatible with zero [10, 11, 12]; however, such a result was obtained on a polarized deuteron target — rather than a hydrogen one, as for HERMES — and the small result could be explained as a cancellation between opposite contributions from u and d quarks. That has allowed the extraction, from data, of the Sivers distribution function [1, 13, 14, 15, 16]. Large SSAs observed in $p^\uparrow p \rightarrow \pi, K + X$ inclusive processes at Fermilab [17, 18, 19] and RHIC [20, 21] could also be explained as a manifestation of the Sivers effect [22, 23, 24]. A recent preliminary result from COMPASS operating on a transversely polarized proton target [25] and still compatible with zero, might, if confirmed, be of difficult interpretation.

From the theoretical point of view the Siverson distribution function [3, 4] had a difficult early life. For some time its very existence was much debated and, despite its phenomenological success [22, 23], fundamental parity and time-reversal properties of QCD seemed to forbid it [26]. Some attempts were made of invoking initial state interactions [23] or unusual time-reversal properties [27]. An explicit model calculation of the Siverson effect in SIDIS [28] much clarified the situation, showing the crucial role of final state interactions. The analysis of Ref. [26] was then reconsidered [29] and the proof that the Siverson asymmetry should vanish because of time-reversal invariance was shown to be invalidated by the path-ordered exponential of the gluon field in the gauge invariant operator definition of parton densities. Thus, the gauge links (gluon exchange in final state interactions) seem to allow a consistent QCD picture of the Siverson effect. The same analysis [29] which led to the conclusion that the Siverson distribution has a full right to existence in QCD, also showed that time-reversal properties imply that the Siverson asymmetry must be *reversed in sign* when acting in SIDIS and Drell-Yan (DY) processes. This was explicitly confirmed by the extension of the model for Siverson effect in SIDIS to the Drell-Yan case [30].

The experimental measurement of the Siverson SSAs in SIDIS and Drell-Yan processes, and the observation of the sign change of the Siverson distribution, is one of the most important tests of our understanding of the origin of SSAs in QCD and the factorization scheme. In this paper we exploit the Siverson functions recently extracted from SIDIS data [1], *change their signs*, and give estimates for Siverson SSAs in Drell-Yan processes; these asymmetries can be measured in several experiments, to be performed at existing facilities (COMPASS, RHIC), developing (J-PARC) or proposed ones (PAX, PANDA, JINR, IHEP).

An early discussion of the contribution of the Siverson function to SSAs in Drell-Yan processes, for RHIC experiments, was presented in Ref. [31]; information on the Siverson distributions was obtained from data on SSAs in inclusive hadronic production, $p^\uparrow p \rightarrow \pi X$, rather than from SIDIS data. This paper updates and extends subsequent studies performed in Refs. [14, 15] and [32]. In Ref. [14] predictions for Siverson SSAs in Drell-Yan processes at RHIC and PAX, based on a first extraction of the Siverson functions from SIDIS data, with no sea contributions, were given. A similar procedure, for RHIC experiments, was followed in Ref. [15]. In Ref. [32] estimates for SSAs at RHIC, PAX (in fixed target mode) and COMPASS were given based on a simple expression of the (opposite) u and d Siverson functions, extracted from a two-parameter fit of the SIDIS HERMES data, and combined with some models for the antiquark Siverson distributions. Here, we use the recent [1], much more structured, valence and sea, Siverson functions obtained from a fit of SIDIS asymmetries for pion and kaon production, measured by HERMES and COMPASS collaborations. We give estimates for the full set of experiments which either have been proposed or are being discussed in many laboratories worldwide.

II. FORMALISM FOR THE SIVERSON EFFECT IN DRELL-YAN PROCESSES

We consider the leading order (LO) parton model cross section for Drell-Yan processes, $A^\uparrow B \rightarrow \ell^+ \ell^- X$ ($A^\uparrow = p^\uparrow$; $B = p, \bar{p}, \pi$), in the hadronic c.m. frame, in which one only observes the four-momentum of the final $\ell^+ \ell^-$ pair, or related quantities:

$$q = (q_0, \mathbf{q}_T, q_L) \quad q^2 = M^2 \quad y = \frac{1}{2} \ln \frac{q_0 + q_L}{q_0 - q_L} \quad x_F = \frac{2q_L}{\sqrt{s}} \quad s = (p_A + p_B)^2. \quad (3)$$

In the kinematical region

$$q_T^2 \ll M^2 \quad k_\perp \simeq q_T, \quad (4)$$

where $q_T = |\mathbf{q}_T|$ and $k_\perp = |\mathbf{k}_\perp|$ is the magnitude of the parton intrinsic motion, at $O(k_\perp/M)$ the Siverson SSA is simply given by [31]

$$A_N = \frac{d\sigma^{A^\uparrow B \rightarrow \ell^+ \ell^- X} - d\sigma^{A^\downarrow B \rightarrow \ell^+ \ell^- X}}{d\sigma^{A^\uparrow B \rightarrow \ell^+ \ell^- X} + d\sigma^{A^\downarrow B \rightarrow \ell^+ \ell^- X}} \equiv \frac{d\sigma^\uparrow - d\sigma^\downarrow}{d\sigma^\uparrow + d\sigma^\downarrow} \quad (5)$$

$$= \frac{\sum_q \int d^2 \mathbf{k}_{\perp 1} d^2 \mathbf{k}_{\perp 2} \delta^2(\mathbf{k}_{\perp 1} + \mathbf{k}_{\perp 2} - \mathbf{q}_T) \Delta^N f_{q/A^\uparrow}(x_1, \mathbf{k}_{\perp 1}) f_{\bar{q}/B}(x_2, \mathbf{k}_{\perp 2}) \hat{\sigma}_0^{q\bar{q}}}{2 \sum_q \int d^2 \mathbf{k}_{\perp 1} d^2 \mathbf{k}_{\perp 2} \delta^2(\mathbf{k}_{\perp 1} + \mathbf{k}_{\perp 2} - \mathbf{q}_T) f_{q/A}(x_1, \mathbf{k}_{\perp 1}) f_{\bar{q}/B}(x_2, \mathbf{k}_{\perp 2}) \hat{\sigma}_0^{q\bar{q}}}, \quad (6)$$

with

$$\hat{\sigma}_0^{q\bar{q}} = e_q^2 \frac{4\pi\alpha^2}{9M^2} \quad x_{1,2} = \frac{M}{\sqrt{s}} e^{\pm y} = \frac{\pm x_F + \sqrt{x_F^2 + 4M^2/s}}{2}, \quad (7)$$

where the subscripts 1 and 2 label the quark and antiquark participating in the elementary LO scattering process, $q\bar{q} \rightarrow \ell^+ \ell^-$. Notice that, with the definition of x_F adopted in Eq. (3), one has

$$x_F = x_1 - x_2 \quad |x_F| \leq 1 - \frac{M^2}{s}. \quad (8)$$

The sum in Eq. (6) runs over all quarks and antiquarks ($q = u, \bar{u}, d, \bar{d}, s, \bar{s}$) and $d\sigma$ stands for

$$\frac{d^4\sigma}{dy dM^2 d^2\mathbf{q}_T} = \frac{1}{s} \frac{d^4\sigma}{dx_1 dx_2 d^2\mathbf{q}_T} = (x_1 + x_2) \frac{d^4\sigma}{dx_F dM^2 d^2\mathbf{q}_T} = \frac{1}{2} \frac{d^4\sigma}{d^4q}. \quad (9)$$

Notice that in obtaining Eq. (6) one uses (see Eq. (1)):

$$\hat{f}_{q/A^\uparrow}(x, \mathbf{k}_\perp) + \hat{f}_{q/A^\downarrow}(x, \mathbf{k}_\perp) = 2 f_{q/A}(x, k_\perp) \quad (10)$$

$$\hat{f}_{q/A^\uparrow}(x, \mathbf{k}_\perp) - \hat{f}_{q/A^\downarrow}(x, \mathbf{k}_\perp) = \Delta^N f_{q/A^\uparrow}(x, k_\perp) \mathbf{S} \cdot (\hat{\mathbf{P}} \times \hat{\mathbf{k}}_\perp) \equiv \Delta^N f_{q/A^\uparrow}(x, \mathbf{k}_\perp). \quad (11)$$

The SSA (6) depends directly on the Sivvers functions $\Delta^N f_{q/A^\uparrow}$.

We use here the same factorized expression of the cross sections which holds in the collinear configuration, generalizing it to the case of unintegrated, or transverse momentum dependent (TMD), partonic distributions [24, 33]. A most general treatment of unpolarized and polarized Drell-Yan processes in such a scheme has very recently appeared [34]. Factorization for SIDIS and Drell-Yan processes in the kinematical regime we are considering here, Eq. (4), has been proven in QCD [35, 36, 37], resulting in the same parton model TMD-factorization adopted here and in Ref. [34], with the addition of an extra soft factor S , which takes into account transverse motion originating from soft gluon emission (see, for example, Eqs. (40) and (41) of Ref. [38]). Such a factor gives an (unknown) additional contribution, both to the numerator and denominator of Eq. (6), of order α_s , and is neglected here. The TMD partonic distributions we use are obtained by fitting experimental data and take into account all sources of intrinsic motion.

A. About sign and azimuthal angle conventions

As the issue of the sign of the Sivvers asymmetry in Drell-Yan processes is so important, let us discuss in details the choices adopted here and their motivation. We define our kinematical configuration with hadron A^\uparrow moving along the positive z -axis, and hadron B opposite to it, in the $A - B$ center of mass frame. We choose the ‘‘up’’ (\uparrow) polarization direction as the positive y -axis ($\phi_S = \pi/2$). The transverse momenta have azimuthal angles

$$\mathbf{q}_T = q_T(\cos \phi_\gamma, \sin \phi_\gamma, 0) \quad \mathbf{k}_{\perp i} = k_{\perp i}(\sin \varphi_i, \cos \varphi_i, 0) \quad (i = 1, 2), \quad (12)$$

so that the mixed product $\mathbf{S} \cdot (\hat{\mathbf{P}} \times \hat{\mathbf{k}}_{\perp 1})$ gives an azimuthal dependence $\sin(\phi_S - \varphi_1) = \cos \varphi_1$ which, upon integration on $\mathbf{k}_{\perp 1}$, yields a $\sin(\phi_S - \phi_\gamma) = \cos \phi_\gamma$ dependence of the Sivvers asymmetry (see Eq. (20) below).

Notice that, contrary to the usual study of angular dependences of Drell-Yan processes which is mainly performed in the so-called Collins-Soper reference frame [39], we work in the hadronic c.m. frame. At least for the purpose of studying the Sivvers asymmetry, this frame is much more convenient and directly related to experimental measurements.

In order to collect data at all azimuthal angles, following what is usually done in semi-inclusive deep inelastic scattering processes, both experimental results and theoretical estimates can be discussed for the azimuthal moments of the asymmetry. We follow Refs. [32, 40] and [15] and choose as a weight the $\sin(\phi_\gamma - \phi_S)$ phase. We then have:

$$\begin{aligned} A_N^{\sin(\phi_\gamma - \phi_S)} &\equiv \frac{\int_0^{2\pi} d\phi_\gamma [d\sigma^\uparrow - d\sigma^\downarrow] \sin(\phi_\gamma - \phi_S)}{\frac{1}{2} \int_0^{2\pi} d\phi_\gamma [d\sigma^\uparrow + d\sigma^\downarrow]} \quad (13) \\ &= \frac{\int d\phi_\gamma \left[\sum_q \int d^2\mathbf{k}_{\perp 1} d^2\mathbf{k}_{\perp 2} \delta^2(\mathbf{k}_{\perp 1} + \mathbf{k}_{\perp 2} - \mathbf{q}_T) \Delta^N f_{q/A^\uparrow}(x_1, \mathbf{k}_{\perp 1}) f_{\bar{q}/B}(x_2, k_{\perp 2}) \hat{\sigma}_0^{q\bar{q}} \right] \sin(\phi_\gamma - \phi_S)}{\int d\phi_\gamma \left[\sum_q \int d^2\mathbf{k}_{\perp 1} d^2\mathbf{k}_{\perp 2} \delta^2(\mathbf{k}_{\perp 1} + \mathbf{k}_{\perp 2} - \mathbf{q}_T) f_{q/A}(x_1, k_{\perp 1}) f_{\bar{q}/B}(x_2, k_{\perp 2}) \hat{\sigma}_0^{q\bar{q}} \right]}. \end{aligned}$$

Notice that such a choice, combined with the $\sin(\phi_S - \phi_\gamma)$ dependence associated with the Sivvers function [see comments following Eq. (12)] implies an overall $[-\sin^2(\phi_\gamma - \phi_S)]$ factor in the numerator of Eq. (13).

The above asymmetry is, in general, a function of x_F (or y), M and q_T . In the sequel we shall study it as a function of one variable only, either x_F or M ; we will always integrate both the numerator and denominator of Eq. (13) over q_T — covering the range in which the factorized approach with unintegrated distribution functions is supposed to hold (as detailed in the captions of Figs. 2-9) — and on one of the remaining variables according to the kinematical ranges of the corresponding experiments.

The case in which the polarized hadron A^\uparrow moves along $-\hat{z}$, that is the process $B A^\uparrow \rightarrow \ell^+ \ell^- X$, deserves a special comment. In such a case — *keeping the same definition of \uparrow polarization and the same reference frame* — the Sivvers mixed product has an opposite sign (due to the opposite A^\uparrow momentum) and yields a Sivvers asymmetry proportional to $\sin(\phi_\gamma - \phi_S)$. In this case the overall factor in the numerator of Eq. (13) is $[\sin^2(\phi_\gamma - \phi_S)]$. This agrees with

what is done in SIDIS processes, $\ell p^\dagger \rightarrow \ell h X$, in the $\gamma^* - p^\dagger$ c.m. frame [5]. To summarize, we shall give estimates for the quantities:

$$A_N^{\sin(\phi_\gamma - \phi_S)}(A^\dagger B \rightarrow \gamma^* X; x_F, M, q_T) = -A_N^{\sin(\phi_\gamma - \phi_S)}(B A^\dagger \rightarrow \gamma^* X; -x_F, M, q_T). \quad (14)$$

The equality holds due to rotational invariance.

III. ESTIMATES FOR FORTHCOMING EXPERIMENTS

In order to give estimates for the Sivers asymmetries in Drell-Yan processes — and test the crucially important sign change when going from SIDIS to DY — we only need to insert the Sivers functions extracted from the analysis of SIDIS data into Eq. (13). We use the results obtained in Ref. [1], which adopted a Gaussian factorized form both for the unpolarized distribution functions:

$$f_{q/p}(x, k_\perp) = f_q(x) \frac{1}{\pi \langle k_\perp^2 \rangle} e^{-k_\perp^2 / \langle k_\perp^2 \rangle} \quad \langle k_\perp^2 \rangle = 0.25 \text{ GeV}^2, \quad (15)$$

and for the Sivers distributions:

$$\begin{aligned} \Delta^N f_{q/p^\dagger}(x, k_\perp) &= 2 \mathcal{N}_q(x) h(k_\perp) f_{q/p}(x, k_\perp) \\ &\equiv \Delta^N f_{q/p^\dagger}(x) h(k_\perp) \frac{1}{\pi \langle k_\perp^2 \rangle} e^{-k_\perp^2 / \langle k_\perp^2 \rangle}, \end{aligned} \quad (16)$$

where

$$\mathcal{N}_q(x) = N_q x^{\alpha_q} (1-x)^{\beta_q} \frac{(\alpha_q + \beta_q)^{(\alpha_q + \beta_q)}}{\alpha_q^{\alpha_q} \beta_q^{\beta_q}} \quad (17)$$

$$h(k_\perp) = \sqrt{2} e \frac{k_\perp}{M_1} e^{-k_\perp^2 / M_1^2}. \quad (18)$$

The values of the 11 best fit parameters N_q ($q = u, d, s, \bar{u}, \bar{d}, \bar{s}$), α_q ($q = u, d, sea$), β (same for all q) and M_1 can be found in Table I of Ref. [1], where their uncertainty is also explained in details.

Notice that the above factorized expressions allow, at $\mathcal{O}(k_\perp/M)$, an analytical integration of the numerator and denominator of Eq. (13), resulting in

$$A_N^{\sin(\phi_\gamma - \phi_S)}(x_F, M, q_T) = \frac{\int d\phi_\gamma [N(x_F, M, q_T, \phi_\gamma)] \sin(\phi_\gamma - \phi_S)}{\int d\phi_\gamma [D(x_F, M, q_T)]} \quad (19)$$

with (see Eq. (9)):

$$\begin{aligned} N(x_F, M, q_T, \phi_\gamma) &\equiv \frac{d^4 \sigma^\uparrow}{dx_F dM^2 d^2 \mathbf{q}_T} - \frac{d^4 \sigma^\downarrow}{dx_F dM^2 d^2 \mathbf{q}_T} \\ &= \frac{4\pi \alpha^2}{9 M^2 s} \sum_q \frac{e_q^2}{x_1 + x_2} \Delta^N f_{q/A^\dagger}(x_1) f_{\bar{q}/B}(x_2) \sqrt{2} e \frac{q_T}{M_1} \frac{\langle k_S^2 \rangle^2 \exp[-q_T^2 / (\langle k_S^2 \rangle + \langle k_{\perp 2}^2 \rangle)]}{\pi [\langle k_S^2 \rangle + \langle k_{\perp 2}^2 \rangle]^2 \langle k_{\perp 2}^2 \rangle} \sin(\phi_S - \phi_\gamma) \end{aligned} \quad (20)$$

and

$$\begin{aligned} D(x_F, M, q_T) &\equiv \frac{1}{2} \left[\frac{d^4 \sigma^\uparrow}{dx_F dM^2 d^2 \mathbf{q}_T} + \frac{d^4 \sigma^\downarrow}{dx_F dM^2 d^2 \mathbf{q}_T} \right] = \frac{d^4 \sigma^{unp}}{dx_F dM^2 d^2 \mathbf{q}_T} \\ &= \frac{4\pi \alpha^2}{9 M^2 s} \sum_q \frac{e_q^2}{x_1 + x_2} f_{q/A}(x_1) f_{\bar{q}/B}(x_2) \frac{\exp[-q_T^2 / (\langle k_{\perp 1}^2 \rangle + \langle k_{\perp 2}^2 \rangle)]}{\pi [\langle k_{\perp 1}^2 \rangle + \langle k_{\perp 2}^2 \rangle]}. \end{aligned} \quad (21)$$

Notice that we have defined

$$\frac{1}{\langle k_S^2 \rangle} = \frac{1}{M_1^2} + \frac{1}{\langle k_{\perp 1}^2 \rangle} \quad (22)$$

and that x_1, x_2 have the values given in Eq. (7). Although in the above equations we have allowed for the possibility of having different values of $\langle k_{\perp 1,2}^2 \rangle$ for hadrons A and B , in our numerical evaluations we shall take them equal, as given by Eq. (15), even when one of the hadrons is a pion.

Our estimates are obtained using, for the proton, the partonic distribution functions (PDF) of Ref. [41] (GRV98LO, consistently with the choice adopted in Ref. [1]) and, for the pion, those of Ref. [42]; all the PDFs are evolved (at LO) at the $Q^2 = M^2$ scale of interest. We have checked that a different choice for the PDFs of the pion [43] yields very similar results for the π^- and results in agreement with those shown here, within the uncertainty bands, for the π^+ . Our results are presented in Figs. 1-9. The shaded bands reflect the statistical uncertainty in the extracted values of the Siverson functions, as explained in Ref. [1]. Let us comment on each figure.

- **Fig. 1**, Siverson functions.

For completeness, the Siverson functions used in this analysis are presented. The sign has been reversed with respect to the Siverson functions obtained from SIDIS data in Ref. [1], according to the findings of Refs. [29, 30]:

$$\Delta^N f_{\text{DY}} = -\Delta^N f_{\text{SIDIS}}. \quad (23)$$

The first moment of the Siverson function, left panel, is defined as:

$$\Delta^N f_{q/p^\uparrow}^{(1)}(x) \equiv \int d^2 \mathbf{k}_\perp \frac{k_\perp}{4m_p} \Delta^N f_{q/p^\uparrow}(x, k_\perp) = -f_{1T}^{\perp(1)q}(x). \quad (24)$$

This quantity is, up to a constant resulting from the $d^2 \mathbf{k}_\perp$ integration, the same as the function $\Delta^N f_{q/A^\uparrow}(x_1)$ appearing in Eqs. (16), (20).

- **Fig. 2**, COMPASS.

$A_N^{\sin(\phi_\gamma - \phi_S)}$ is shown as a function of $x_F = x_1 - x_2$, left plot, and of M , central plot, for the COMPASS planned experiment, $\pi^\pm p^\uparrow \rightarrow \mu^\pm \mu^- X$. We have integrated both the numerator and denominator of Eq. (19) over q_T in the range $(0 \leq q_T \leq 1)$ GeV, which is within the region of validity of our approach. The other integration ranges are $(4 \leq M \leq 9)$ GeV, at fixed x_F , for the left plot and $0.2 \leq x_F \leq 0.5$, at fixed M , for the central plot. The pion beam energy, in the laboratory frame, is taken to be 160 GeV, corresponding to $\sqrt{s} = 17.4$ GeV.

In the right panel we show the kinematical region covered by the COMPASS experiment, *i.e.* the range of allowed x_2 values, which refer to the polarized proton distributions, as a function of x_F . It is interesting to notice that positive values of x_F correspond to (or at least overlap with) the x region explored by the SIDIS experiments ($x \leq 0.35$) and the data used to extract our Siverson functions. Instead, negative values of x_F correspond to larger x_2 values, a region yet unexplored by other experiments, so that our estimates are based on the assumed functional form of the Siverson function — not constrained, in that region, by any SIDIS data — and are bound to have much larger uncertainties.

Finally, it is important to remark that, as the COMPASS experiment will involve charged pion beams, $\pi^-(\bar{u}d)$ and $\pi^+(u\bar{d})$, the dominant elementary process contributing to the asymmetry will be $\bar{u}_{\pi^-} u_p \rightarrow \mu^+ \mu^-$ for the π^- beam and $\bar{d}_{\pi^+} d_p \rightarrow \mu^+ \mu^-$ for the π^+ beam. Consequently, the prediction of the sign change of the Siverson function in SIDIS and Drell-Yan processes [29, 30] can be clearly tested, as the sign of the asymmetry for π^- (π^+) beam is given by the sign of the u (d) Siverson function, which is well established.

- **Fig. 3**, COMPASS (low M).

We show our estimates for the single spin asymmetry and the corresponding allowed kinematical region in the $x_2 - x_F$ plane, for COMPASS experiments performed at lower M values, $(2.0 \leq M \leq 2.5)$ GeV and in a more limited q_T region, $(0 \leq q_T \leq 0.4)$ GeV (so that the constraints of Eq. (4) remain true). This exploits the possibility of DY measurements in the low mass region, below the J/ψ and above the ρ resonance peaks, where data should be much more abundant.

- **Fig. 4**, RHIC.

$A_N^{\sin(\phi_\gamma - \phi_S)}$ is shown as a function of x_F and M for RHIC experiments, $p^\uparrow p \rightarrow \ell^+ \ell^- X$, at $\sqrt{s} = 200$ GeV. The integration ranges for q_T and M are the same as in Fig. 2, with the further constraint $0 \leq y \leq 3$, according to the experimental kinematical cuts. The right panel shows the kinematical region of RHIC for x_1 as a function of x_F . This region covers the range already explored by SIDIS measurements ($x \leq 0.35$) where the Siverson functions are reliably constrained, and expands into much higher values of x . The maximum value of the asymmetry ($\sim 10\%$) shown in the left panel is expected at $x_F \simeq 0.2$ which corresponds (see the right panel) to $x_1 \simeq 0.2$, where the valence Siverson functions reach their maximum, see Fig. 1.

The asymmetry for larger values of x_F (> 0.4) is obtained by using our extracted Siverson functions at large values of x where SIDIS data offer no constraint. This reflects into the huge uncertainty band. Let us remind that in Ref. [1] we have assumed the β parameters, which determine the large x behaviour of the Siverson functions, to be equal for all flavours. With such an assumption the asymmetry decreases fast for high values of x_F , although with a large uncertainty. The parameterization of our previous analysis [14], where β_u and β_d were different for u and d flavours, would lead to a larger asymmetry at high x_F (see Fig. 6 of Ref. [14]). Measurements in the region of high x_F could then offer an opportunity to test the flavour-blind β assumption. Moreover, data in the negative x_F region would test the contribution of the sea Siverson functions, as first pointed out in Ref. [32].

- **Fig. 5, PAX.**

Estimates are given for the planned GSI-PAX experiment [44], $p^\uparrow\bar{p} \rightarrow \ell^+\ell^-X$, in the asymmetric collider mode at $\sqrt{s} = 14.14$ GeV, with a polarized proton beam. This experiment would have the big advantage of having proton and antiproton beams, thus increasing the number of Drell-Yan events. $A_N^{\sin(\phi_\gamma - \phi_S)}$ is shown as a function of x_F (integrating over $(4 \leq M \leq 6)$ GeV, with the constraint $|y| < 1$), and as a function of M (integrating over x_F with $|y| < 1$); in both cases q_T is integrated in the range $(0 \leq q_T \leq 1)$ GeV.

The negative x_F region gets most contribution from the valence x_1 region, which is well explored by SIDIS experiments and where the Siverson distributions are reliably known. In this region the asymmetry is large (10-15% in size) and sensitive only to the u and d Siverson functions. On the contrary, at large and positive x_F values the situation becomes similar to that described for RHIC, as we need the Siverson functions in the large x -range, which are more poorly known. Once again, this results in large uncertainties of our estimates.

The PAX collaboration aims at having a beam of polarized antiprotons, which, in combination with a beam of polarized protons, would allow a unique direct way of measuring the transversity distributions [44]. In such a case, one could also measure the single spin Siverson asymmetry in the process $p\bar{p}^\uparrow \rightarrow \ell^+\ell^-X$; this is related to the one considered here by charge conjugation invariance and the relation of Eq. (14),

$$A_N^{\sin(\phi_\gamma - \phi_S)}(p\bar{p}^\uparrow \rightarrow \gamma^*X; x_F, M, q_T) = -A_N^{\sin(\phi_\gamma - \phi_S)}(p^\uparrow\bar{p} \rightarrow \gamma^*X; -x_F, M, q_T). \quad (25)$$

- **Fig. 6, PANDA.**

The GSI-PANDA experiment [45] will run with an antiproton beam scattering off a proton target, at the energy $E_{\bar{p}} = 15$ GeV, corresponding to $\sqrt{s} = 5.47$ GeV. It might be worth trying to have a polarized target, $\bar{p}p^\uparrow \rightarrow \ell^+\ell^-X$. We then show predictions for $A_N^{\sin(\phi_\gamma - \phi_S)}$ as a function of x_F ; the integration ranges, due to the moderate energy, are $(2.0 \leq M \leq 2.5)$ GeV and $(0 \leq q_T \leq 0.4)$ GeV. The kinematical range which could be explored is entirely overlapping with that covered by the SIDIS data, so that this experiment would supply a perfect consistency check of the HERMES and COMPASS results, and of the crucial Eq. (23). The asymmetry turns out to be sizable and well definite in sign over the full kinematical range.

- **Fig. 7, J-PARC.**

J-PARC might measure Drell-Yan single spin asymmetries $A_N^{\sin(\phi_\gamma - \phi_S)}$ generated in polarized proton-proton collisions at $E_p = 50$ GeV [46], corresponding to $\sqrt{s} = 9.78$ GeV (see the figure caption for further information). As shown on the right panel, the kinematical range covered by J-PARC would be almost entirely complementary to that explored in the SIDIS experiments. These measurements could then be of great importance to obtain information on the large- x behaviour of the Siverson distribution functions.

- **Fig. 8, NICA.**

NICA is a planned Drell-Yan experiment to be performed at JINR in Dubna [47]. We present our estimates for an unpolarized proton beam scattering off polarized protons at $\sqrt{s} = 20$ GeV. As shown in the right panel, the region of large and negative x_F (< -0.5) corresponds to the range of x_2 values for which we have no information from SIDIS experiments. Therefore the measurements of $A_N^{\sin(\phi_\gamma - \phi_S)}$ in this region would provide information on the large x behaviour of the Siverson functions. Our results have smaller uncertainties in the region $-0.4 \lesssim x_F \lesssim 0.1$ which corresponds to the x_2 valence region and where the asymmetry is related to the convolution $4f_{\bar{u}} \otimes \Delta^N f_u + f_{\bar{d}} \otimes \Delta^N f_d$. The comparison between the left and the central plots shows that the positive x_F region is dominated by the Siverson sea contribution. More information can be found in the figure caption.

- **Fig. 9, SPASCHARM.**

The SPASCHARM experiment [48] at IHEP in Protvino (Russia) plans to measure Drell-Yan processes both in polarized proton-proton scattering at $P_{\text{Lab}} = 60$ GeV, corresponding to $\sqrt{s} = 10.7$ GeV (upper panels) and

in pion-proton scattering at $E_\pi = 34$ GeV, corresponding to $\sqrt{s} = 8$ GeV (lower panels). SPASCHARM would mainly collect data in the range of low values of M [$2.0 \leq M \leq 2.5$] GeV and in the valence region of the Sivers functions (see the figure caption for more details). Therefore, SPASCHARM measurements of pion-proton asymmetries, like the analogous COMPASS case, could provide a stringent test of the sign change of the Sivers function in Drell-Yan and SIDIS processes.

IV. COMMENTS AND CONCLUSIONS

We have given clear and simple estimates of Sivers SSAs in Drell-Yan processes, which could be measured in experiments which are either in preparation or being planned. Our results show large values of these asymmetries, which, despite the uncertainty in magnitude related to the extraction of the Sivers functions from SIDIS data, have an unambiguous sign. This sign originates from the current understanding of the origin of SSAs at the partonic level [29] which predicts that the Sivers distributions must enter with opposite signs in SIDIS and Drell-Yan processes. Then, the mere measurement of this sign would, alone, provide a stringent and important test of the present interpretation of the observed SSAs in terms of TMD distribution functions, coupled to initial or final state QCD interactions.

This test, if successful, would be a significant and decisive step towards a basic and consistent description of subtle phenomena like the challenging SSAs in terms of elementary pQCD dynamics and fundamental properties of the nucleon structure involving quark intrinsic motion. Drell-Yan processes at small q_T values, exploring the quark content of the nucleon without the complications of fragmentation processes, might play a crucial role in the future exploration of the proton structure.

Acknowledgements

We acknowledge support of the European Community - Research Infrastructure Activity under the FP6 “Structuring the European Research Area” program (HadronPhysics, contract number RII3-CT-2004-506078). M.A., M.B., and A.P. acknowledge partial support by MIUR under Cofinanziamento PRIN 2006. This work is partially supported by the Helmholtz Association through funds provided to the virtual institute “Spin and strong QCD” (VH-VI-231).

-
- [1] M. Anselmino, et al., *Eur. Phys. J.* **A39**, 89 (2009), arXiv:0805.2677 [hep-ph].
 - [2] G. L. Kane, J. Pumplin, and W. Repko, *Phys. Rev. Lett.* **41**, 1689 (1978).
 - [3] D. W. Sivers, *Phys. Rev.* **D41**, 83 (1990).
 - [4] D. W. Sivers, *Phys. Rev.* **D43**, 261 (1991).
 - [5] A. Bacchetta, U. D’Alesio, M. Diehl, and C. A. Miller, *Phys. Rev.* **D70**, 117504 (2004), arXiv:hep-ph/0410050.
 - [6] D. Sivers, *Phys. Rev.* **D74**, 094008 (2006), arXiv:hep-ph/0609080.
 - [7] M. Burkardt, and G. Schnell, *Phys. Rev.* **D74**, 013002 (2006), arXiv:hep-ph/0510249.
 - [8] A. Airapetian, et al. (HERMES), *Phys. Rev. Lett.* **94**, 012002 (2005), arXiv:hep-ex/0408013.
 - [9] M. Diefenthaler (HERMES), arXiv:0706.2242 [hep-ex].
 - [10] V. Y. Alexakhin, et al. (COMPASS), *Phys. Rev. Lett.* **94**, 202002 (2005), arXiv:hep-ex/0503002.
 - [11] A. Martin (COMPASS), *Czech. J. Phys.* **56**, F33 (2006), arXiv:hep-ex/0702002.
 - [12] M. Alekseev, et al. (COMPASS), arXiv:0802.2160 [hep-ex].
 - [13] M. Anselmino, et al., *Phys. Rev.* **D71**, 074006 (2005), arXiv:hep-ph/0501196.
 - [14] M. Anselmino, et al., *Phys. Rev.* **D72**, 094007 (2005), arXiv:hep-ph/0507181.
 - [15] W. Vogelsang, and F. Yuan, *Phys. Rev.* **D72**, 054028 (2005), arXiv:hep-ph/0507266.
 - [16] J. C. Collins, et al., *Phys. Rev.* **D73**, 014021 (2006), arXiv:hep-ph/0509076.
 - [17] D. L. Adams, et al. (E581) *Phys. Lett.* **B261**, 197 (1991).
 - [18] D. L. Adams, et al. (E704) *Phys. Lett.* **B264**, 462 (1991).
 - [19] D. L. Adams, et al. (E704) *Phys. Lett.* **B345**, 569 (1995).
 - [20] J. Adams, et al. (STAR) *Phys. Rev. Lett.* **92**, 171801 (2004), arXiv:hep-ex/0310058.
 - [21] I. Arsene, et al. (BRAHMS) *Phys. Rev. Lett.* **101**, 042001 (2008), arXiv:0801.1078 [nucl-ex].
 - [22] M. Anselmino, M. Boggione, and F. Murgia, *Phys. Lett.* **B362**, 164 (1995), arXiv:hep-ph/9503290.
 - [23] M. Anselmino, and F. Murgia, *Phys. Lett.* **B442**, 470 (1998), arXiv:hep-ph/9808426.
 - [24] U. D’Alesio, and F. Murgia, *Phys. Rev.* **D70**, 074009 (2004), arXiv:hep-ph/0408092.
 - [25] S. Levorato (COMPASS), arXiv:0808.0086 [hep-ex].
 - [26] J. C. Collins, *Nucl. Phys.* **B396**, 161 (1993).
 - [27] M. Anselmino, V. Barone, A. Drago, and F. Murgia, *Nucl. Phys. Proc. Suppl.* **105**, 132 (2002), arXiv:hep-ph/0111044.

- [28] S. J. Brodsky, D. S. Hwang, and I. Schmidt, *Phys. Lett.* **B530**, 99 (2002), arXiv:hep-ph/0201296.
- [29] J. C. Collins, *Phys. Lett.* **B536**, 43 (2002), arXiv:hep-ph/0204004.
- [30] S. J. Brodsky, D. S. Hwang, and I. Schmidt, *Nucl. Phys.* **B642**, 344 (2002), arXiv:hep-ph/0206259.
- [31] M. Anselmino, U. D'Alesio, and F. Murgia, *Phys. Rev.* **D67**, 074010 (2003), arXiv:hep-ph/0210371.
- [32] J. C. Collins, et al., *Phys. Rev.* **D73**, 094023 (2006), arXiv:hep-ph/0511272.
- [33] U. D'Alesio, and F. Murgia, *Prog. Part. Nucl. Phys.* **61** **2008**, 394 (2008), arXiv:0712.4328 [hep-ph].
- [34] S. Arnold, A. Metz, and M. Schlegel (2008), arXiv:0809.2262 [hep-ph].
- [35] J. C. Collins, D. E. Soper, and G. Sterman, *Nucl. Phys.* **B250**, 199 (1985).
- [36] X.-d. Ji, J.-p. Ma, and F. Yuan, *Phys. Rev.* **D71**, 034005 (2005), arXiv:hep-ph/0404183.
- [37] X.-d. Ji, J.-P. Ma, and F. Yuan, *Phys. Lett.* **B597**, 299 (2004), arXiv:hep-ph/0405085.
- [38] X. Ji, J.-w. Qiu, W. Vogelsang, and F. Yuan, *Phys. Rev.* **D73**, 094017 (2006), arXiv:hep-ph/0604023.
- [39] J. C. Collins, and D. E. Soper, *Phys. Rev.* **D16**, 2219 (1977).
- [40] A. V. Efremov, K. Goeke, S. Menzel, A. Metz, and P. Schweitzer, *Phys. Lett.* **B612**, 233 (2005), arXiv:hep-ph/0412353.
- [41] M. Gluck, E. Reya, and A. Vogt, *Eur. Phys. J.* **C5**, 461 (1998), arXiv:hep-ph/9806404.
- [42] M. Gluck, E. Reya, and A. Vogt, *Z. Phys.* **C53**, 127 (1992).
- [43] P. J. Sutton, A. D. Martin, R. G. Roberts, and W. J. Stirling, *Phys. Rev.* **D45**, 2349 (1992).
- [44] V. Barone, et al. (PAX), arXiv:hep-ex/0505054.
- [45] K. T. Brinkmann (PANDA), *Nucl. Phys.* **A790**, 75 (2007).
- [46] D. Dutta, et al., J-PARC Letter of Intent L15, URL: <http://psux1.kek.jp/jhf-np/LOIlist/LOIlist.html>
- [47] G. V. Trubnikov, et al. (NICA), *11th European Particle Accelerator Conference (EPAC 08)*, Genoa, Italy, 23-27 June 2008, URL: <http://accelconf.web.cern.ch/AccelConf/e08/papers/wepp029.pdf>
- [48] A. N. Vasiliev, et al., *Proceedings of the XII Workshop on High Energy Spin Physics, DSPIN-07*, p. 368 (Dubna, Russia, September 3-7, 2007), arXiv:hep-ex/0712.2691.

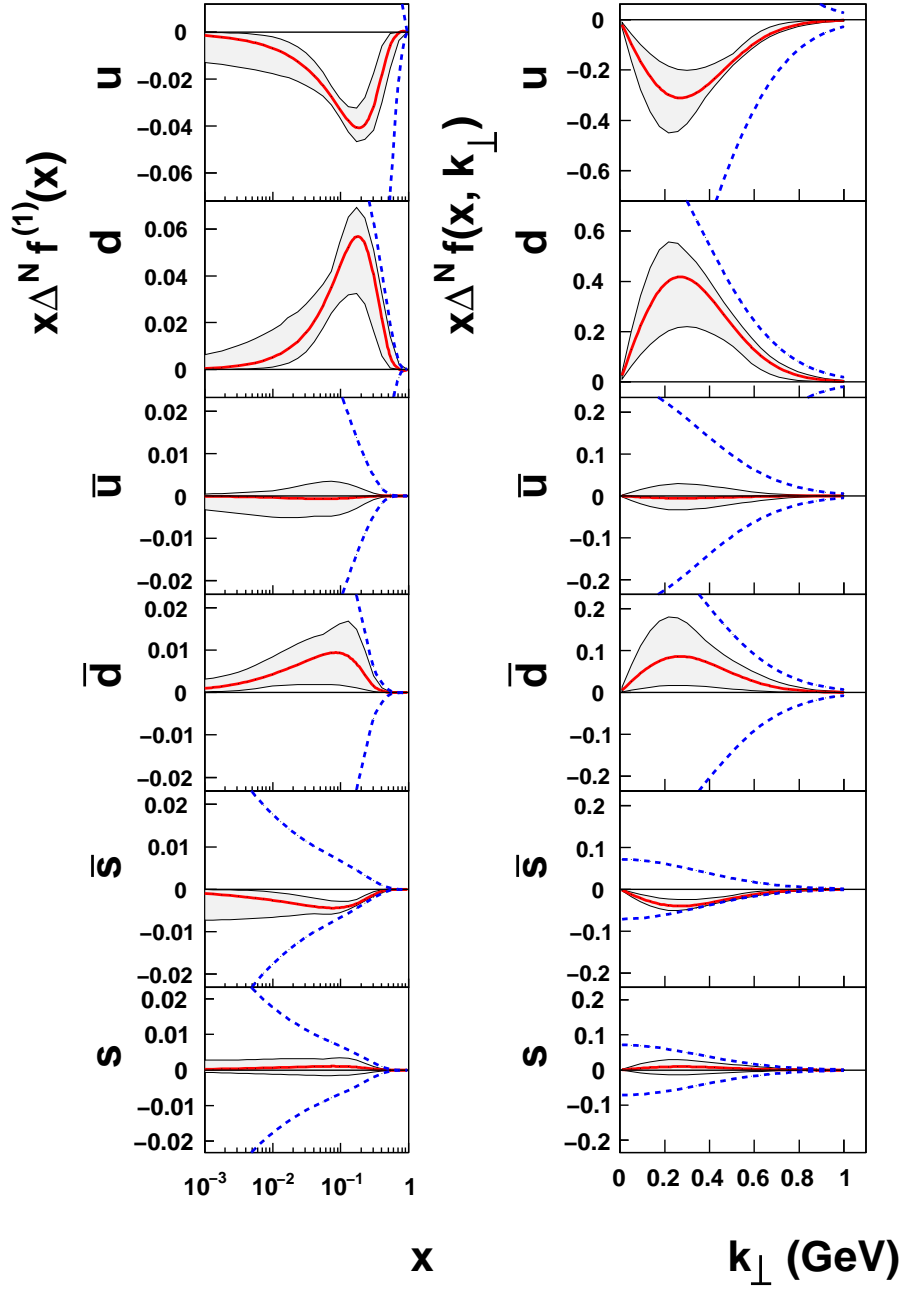


FIG. 1: The Siverts distribution functions for u , d and s flavours as determined by our simultaneous fit of HERMES and COMPASS data in Ref. [1]. The sign was reversed according to the prediction of Refs. [29, 30]. On the left panel, the first moment, $x \Delta^N f^{(1)}(x)$, is shown as a function of x at $Q^2 = 2.4 \text{ GeV}^2$ for each flavour. On the right panel, the Siverts distribution, $x \Delta^N f(x, k_{\perp})$, is shown as a function of k_{\perp} at a fixed value of $x = 0.1$ for each flavour. In each plot, the highest and lowest dashed lines show the positivity limits $|\Delta^N f| = 2f$.

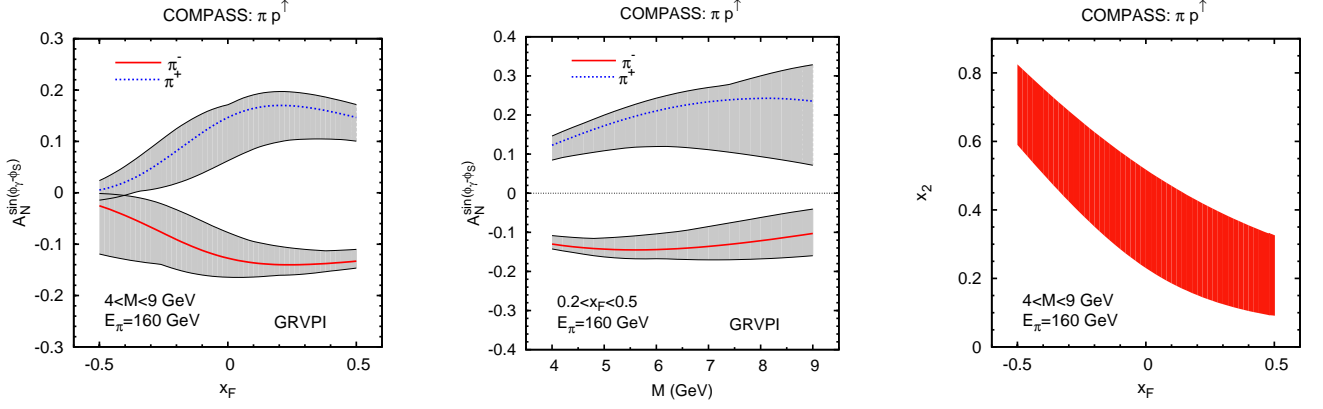


FIG. 2: The single spin asymmetries $A_N^{\sin(\phi_\gamma - \phi_S)}$ for the Drell-Yan process $\pi^\pm p^\uparrow \rightarrow \mu^+ \mu^- X$ at COMPASS, as a function of $x_F = x_1 - x_2$ (left panel) and as a function of M (central panel). The integration ranges are $(0 \leq q_T \leq 1)$ GeV, $(4 \leq M \leq 9)$ GeV and $0.2 \leq x_F \leq 0.5$. The results are given for a pion beam energy of 160 GeV, corresponding to $\sqrt{s} = 17.4$ GeV. The right panel shows the allowed region of x_2 values as a function of x_F .

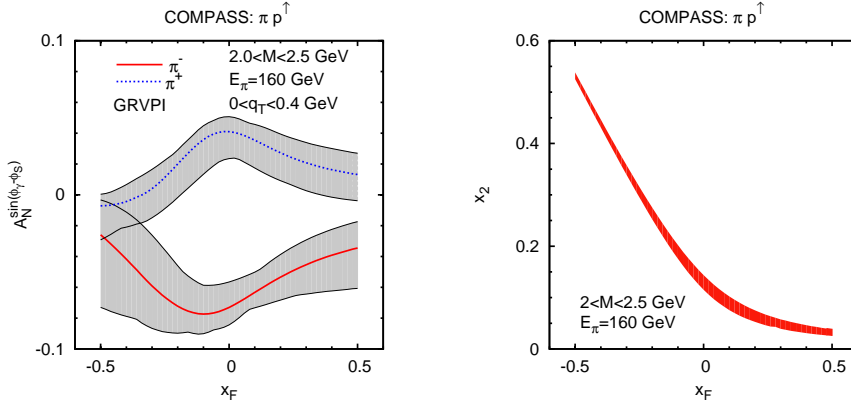


FIG. 3: The single spin asymmetries $A_N^{\sin(\phi_\gamma - \phi_S)}$ for the Drell-Yan process $\pi^\pm p^\uparrow \rightarrow \mu^+ \mu^- X$ at COMPASS, as a function of $x_F = x_1 - x_2$ (left panel). The integration ranges are $(0 \leq q_T \leq 0.4)$ GeV and $(2.0 \leq M \leq 2.5)$ GeV. The results are given for a pion beam energy of 160 GeV, corresponding to $\sqrt{s} = 17.4$ GeV. The right panel shows the allowed region of x_2 values as a function of x_F .

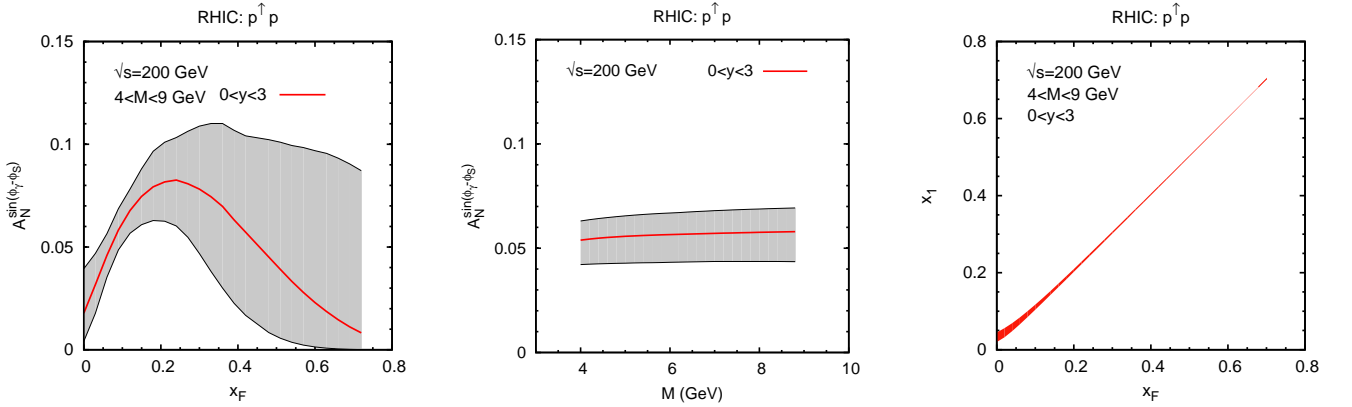


FIG. 4: The single spin asymmetry $A_N^{\sin(\phi_\gamma - \phi_S)}$ for the Drell-Yan process $p^\uparrow p \rightarrow \mu^+ \mu^- X$ at RHIC, as a function of x_F (left panel) and M (central panel). The integration ranges are $(0 \leq q_T \leq 1)$ GeV and $(4 \leq M \leq 9)$ GeV, with the further constraint $0 \leq y \leq 3$. The results are given at $\sqrt{s} = 200$ GeV. The right panel shows the allowed region of x_1 values as a function of x_F .

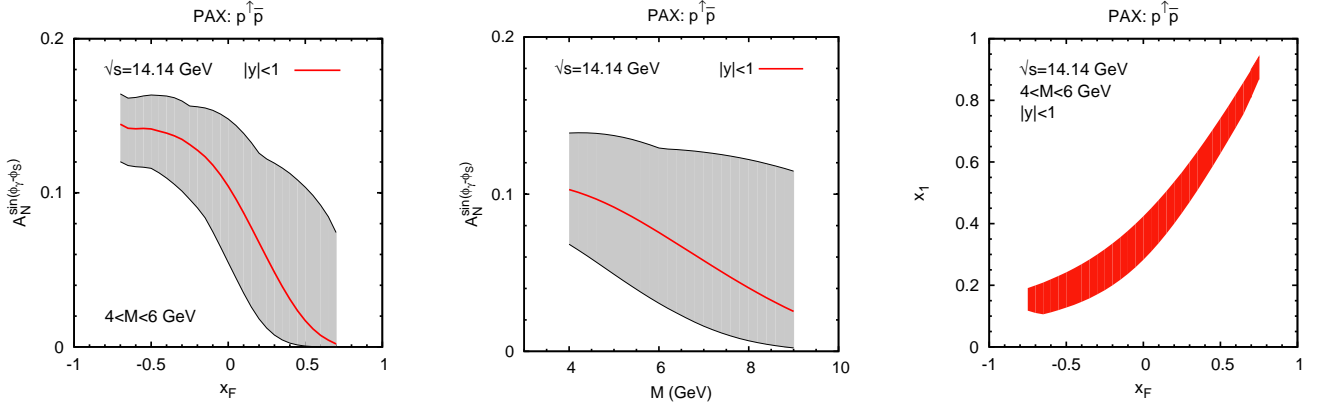


FIG. 5: The single spin asymmetry $A_N^{\sin(\phi_\gamma - \phi_S)}$ for the Drell-Yan process $p^\uparrow \bar{p} \rightarrow \mu^+ \mu^- X$ at PAX, as a function of x_F (left panel) and M (central panel). The integration ranges are $(0 \leq q_T \leq 1)$ GeV and $(4 \leq M \leq 6)$ GeV with the further constraint $|y| \leq 1$. The results are given at $\sqrt{s} = 14.14$ GeV. The right panel shows the allowed region of x_1 values as a function of x_F .

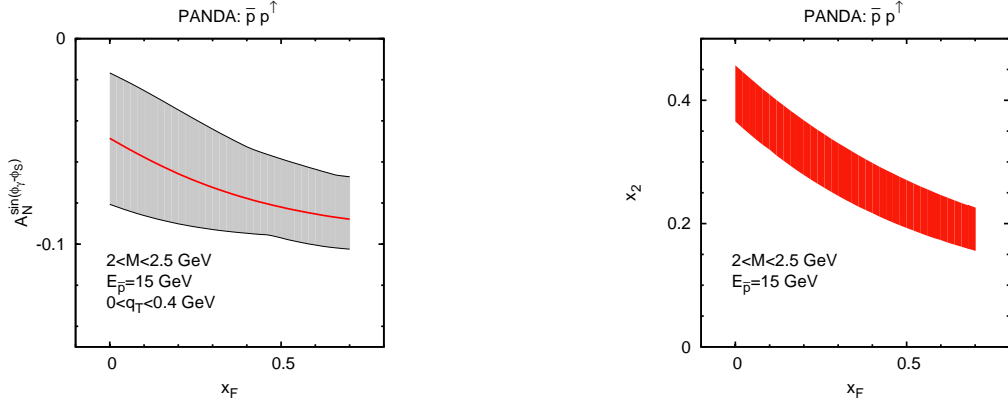


FIG. 6: The single spin asymmetry $A_N^{\sin(\phi_\gamma - \phi_S)}$ for the Drell-Yan process $\bar{p} p^\uparrow \rightarrow \mu^+ \mu^- X$ at PANDA, as a function of x_F . The integration ranges are $(0 \leq q_T \leq 0.4)$ GeV and $(2 \leq M \leq 2.5)$ GeV. The right panel shows the allowed region of x_2 values as a function of x_F . The results are given at $E_{\bar{p}} = 15$ GeV, corresponding to $\sqrt{s} = 5.47$ GeV.

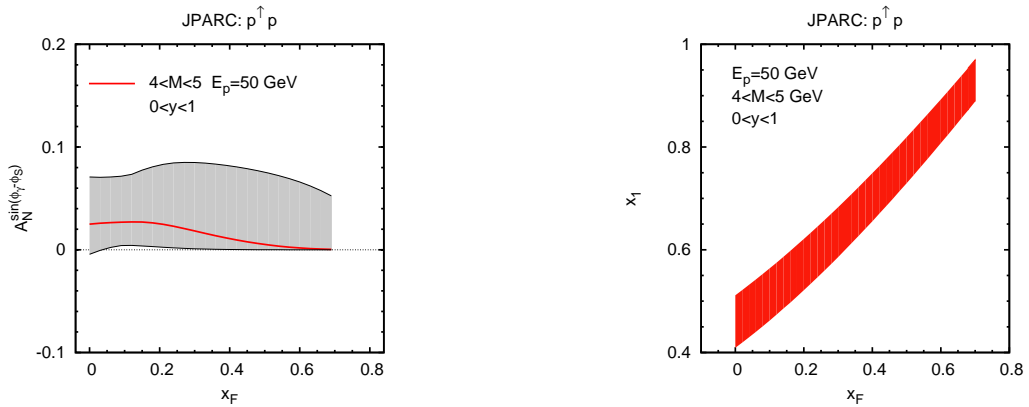


FIG. 7: The single spin asymmetry $A_N^{\sin(\phi_\gamma - \phi_S)}$ for the Drell-Yan process $p^\uparrow p \rightarrow \mu^+ \mu^- X$ at J-PARC, as a function of x_F . The integration ranges are $(0 \leq q_T \leq 1)$ GeV and $(4 \leq M \leq 5)$ GeV. The results are given at $E_p = 50$ GeV, corresponding to $\sqrt{s} = 9.78$ GeV. The right panel shows the allowed region of x_1 values as a function of x_F .

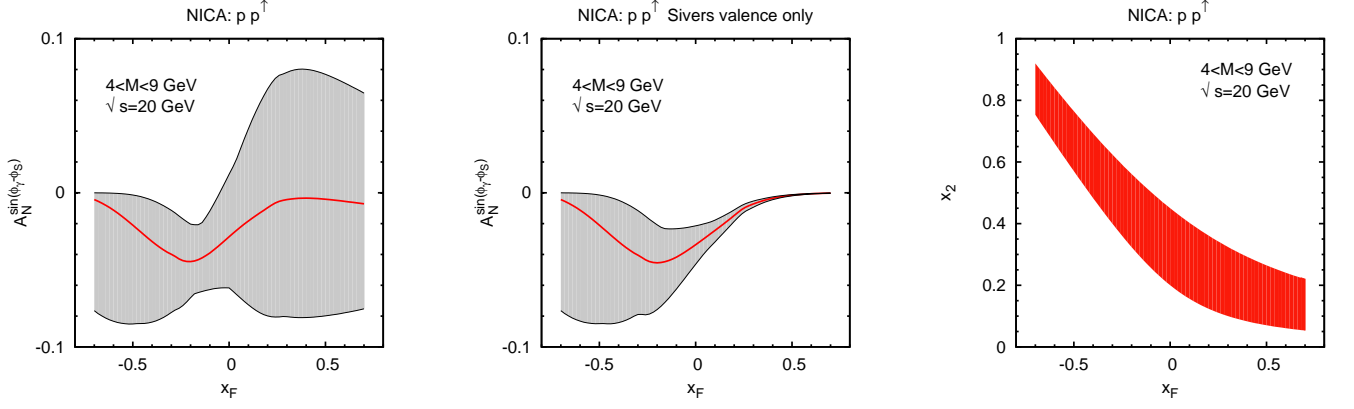


FIG. 8: The single spin asymmetry $A_N^{\sin(\phi_\gamma - \phi_S)}$ for the Drell-Yan process $pp^\uparrow \rightarrow \mu^+\mu^- X$ at JINR (NICA experiment), as a function of x_F . The integration ranges are $(0 \leq q_T \leq 1)$ GeV and $(4 \leq M \leq 9)$ GeV. The results are given at $\sqrt{s} = 20$ GeV; on the left panel we include the Siverson sea contributions, while on the central panel we show the results we obtain by including only the Siverson valence functions. The right panel shows the allowed region of x_2 values as a function of x_F .

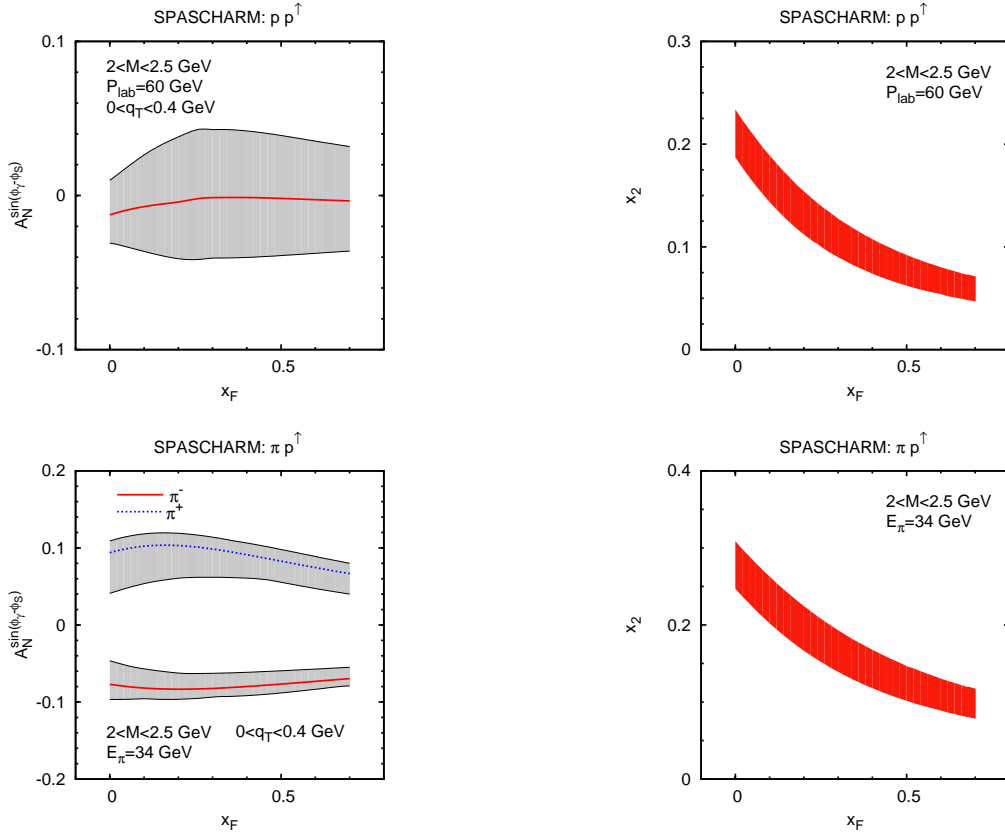


FIG. 9: The single spin asymmetries $A_N^{\sin(\phi_\gamma - \phi_S)}$ for the Drell-Yan process $pp^\uparrow \rightarrow \mu^+\mu^- X$ (upper-left panel) and $\pi p^\uparrow \rightarrow \mu^+\mu^- X$ (lower-left panel) at IHEP (SPASCHARM experiment), as a function of x_F . The integration ranges are $(0 \leq q_T \leq 0.4)$ GeV and $(2 \leq M \leq 2.5)$ GeV. The energies of the two experiments are, respectively, $P_{\text{lab}} = 60$ GeV, corresponding to $\sqrt{s} = 10.7$ GeV, and $E_\pi = 34$ GeV, corresponding to $\sqrt{s} = 8$ GeV. The right panels show the allowed region of x_2 values as a function of x_F .